# A Phenomenological Model for Surface Diffusion: Diffusive Dynamics across Incoherent Stochastic Aperiodic Potentials

**Jeremy M. Moix, Tricia D. Shepherd,† and Rigoberto Hernandez***

*Center for Computational Molecular Science and Technology, School of Chemistry and Biochemistry, Georgia Institute of Technology, Atlanta, Georgia 30332-0400*

*Received: July 28, 2004; In Final Form: September 17, 2004*

The dynamics of Brownian particles diffusing across a one-dimensional, incoherent stochastic potential of mean force in the Smoluchowski regime has been intensely investigated by several groups. In recent work, we have developed a phenomenological equation of motion that extends this representation throughout the friction regime and, in particular, extends it to the low-friction regime relevant to surface diffusion. Resonant activation is observed throughout; it is manifested by a peak in the transport as a function of the correlation time in the potential fluctuations. The phenomenological equation of motion has now been utilized to probe the dynamics on a variety of one- and two-dimensional surfaces in order to provide a qualitative description of the fundamental factors that govern the surface hopping events of an adsorbate weakly bound to a metal surface. The primary focus is placed on differences that may arise when the substrate is modeled using a one- or two-dimensional potential of mean force, thereafter the effects of spatially coherent or incoherent barrier heights are also addressed. The two-dimensional behavior can be adequately described by the direct product of two separable one-dimensional analogues, as might naïvely be expected, provided the lattice spacing is sufficient to decouple the two degrees of freedom. Coherency between the barriers affects the rates to a smaller degree and is significant only when the barriers are strongly correlated in time.

## I. Introduction

Describing the diffusive motion of an adsorbate on a metal surface has recently become an area of intense study, both theoretically and experimentally,[1−8] as it is one of the most fundamental processes in solid-state physics, with applications to catalysis, molecular self-assembly, and numerous others. Accurate experimental measurements, obtained via scanning tunneling or atomic force microscopies, are exceedingly difficult because they require both time- and lattice-resolved measurements over a large area of the surface.[5,9−11] From a theoretical standpoint, the situation is equally difficult. Modeling surface diffusion remains an overwhelming task due not only to the large number of degrees of freedom present in the system but also to the multiple time scales involved in the process. In order to properly simulate these dynamics, the coupled motions of the adsorbate, surface atoms, and the bulk atoms must all be taken into account. As a first approximation to cope with this complexity, one can generally treat these motions separately because they evolve on such differing time scales, by coupling the primary dynamical process of interest to an external bath whose mean properties are capable of accounting for all of the other molecules in an average way. The details of the very small time-scale dynamics associated with electron−hole pair excitation processes are subsumed within this external bath, though in the future they might be included within a larger hierarchy of time scale events. The resulting process is characterized by a stochastic, Langevin equation of motion.[12] The use of a phenomenological equation such as this arises out of necessity, rather than desirability, due to the presence of a large number of degrees of freedom that would otherwise require an analytically intractable or numerically unfeasible number of equations of motion.

In a previous study, a naïve stochastic model was formulated that may be capable of describing the underlying dynamics of an adatom in the low-friction regime.[13] This extension is essential to accurately account for the weak interaction of the adsorbate with the surface, as has been verified by several experiments.[5,14] Theoretical efforts have been able to qualitatively reproduce experimental data by employing a periodic lattice of the same form as the atomic unit cell.[12,15,16] As an extension to these models for the substrate, we have previously utilized a periodic, stochastic potential of mean force such that the barriers are no longer fixed.[13] This inclusion enables the equation of motion to account for both the electronic structure and the time-dependent nature of the surface provided that its statistical properties are known. Additionally, some peculiarities have been noted with this class of stochastic potentials.[17−19] In particular, the rate of diffusion across the surface is heavily dependent upon the fluctuations of the barriers leading to a maximum in the rate of transport when the inherent time scale of the dynamics is of the same order as these fluctuations. This phenomenon, which was first termed "stochastic resonance" in a model for climatic changes[17] when the driving potential is deterministic (and likely periodic) and later[18] "resonant activation" when the potential is nondetermistic, has been the subject of considerable research over the past decade and is the primary motivation for this work.[17−24]

The ultimate goal herein lies in the possibility of providing a novel means for patterning a surface at the atomic level. Theoretically, it has been shown that the stochastic resonance persists in two dimensions when the process is driven by an

* To whom correspondence should be addressed. E-mail: hernandez@chemistry.gatech.edu.

† Present address: 224 Malouf Hall, Westminster College, Salt Lake City, UT 84105.

10.1021/jp046629w CCC: $27.50 
Published on Web 11/20/2004

external field.[25] Additionally, we have shown that if one can instead introduce internal fluctuations into a one-dimensional surface, then it is possible to enhance the diffusion of adsorbates.[13] Experiments have proven that electron and photon bombardment of surfaces can enhance adsorbate diffusion.[26,27] It has also been shown recently through a series of experiments that the electric field produced by a scanning tunneling microscope can stimulate adatom diffusion toward the area around the tip on a room-temperature metal surface and that this can be done in a nonuniform manner leading to the formation of complex structures at the subnanometer scale.[28−30] Here, we propose a more general mechanism based upon resonant activation that can be used to control the diffusive behavior in a less intensive manner by stimulating the surface on a broad scale. If one could further obtain some spatial control over these fluctuations, then it is conceivable that one could pattern a surface in any way desired in a nondestructive manner using the intrinsic properties of the surface to guide the path of the adsorbate.

In the present case, we have extended the phenomenological equation of motion to include two-dimensional, stochastic potentials as a first step toward a more realistic model of the adatom dynamics as well as to provide fundamental insights into the mechanisms governing these systems. Will nontrivial effects arise due to coupling between the spatial degrees of freedom? Recent evidence from several experiments has concluded that diffusion processes involve multiple, complex hopping mechanisms to both nearest and nonnearest neighbors, which suggest that it is possible.[5,10,14] For example, it has been proposed that an adatom that originally traverses linearly along one direction may later change its course during its interactions with the surface and diffuse along the other.[10] In this case, a one-dimensional potential will never be capable of modeling the dynamics properly. The results shown here are in agreement with this picture in that the two-dimensional transport properties are found to be nontrivially related to the corresponding one-dimensional results.

In section II, the heuristic construction of the equation of motion for an underdamped particle experiencing a stochastic potential is presented as well as a brief description of the characterization of the hopping process. Section III presents a comparison of the dynamics seen on two different variants of the two-dimensional surface and their corresponding one-dimensional counterparts. As in earlier work, the numerical rates obtained for a surface at the limits of the correlation time in the stochastic potential are computed as a verification for the intermediate regimes.

## II. Model and Methods

The diffusive behavior of a Brownian particle traversing a stochastic potential is governed by the Langevin equation (LE)

$$\dot{v} = -\gamma v + \xi(t) + F(q;t), \tag{1}$$

where $v = \dot{q}$ is the velocity of the particle, $\gamma$ is the friction constant, and $F(q,t)$ is a stochastic external force. For clarity, the mass of the particle has been set to unity through a canonical transformation but is readily included. The thermal fluctuations present in the system are described by $\xi(t)$ and are treated in the standard manner as a Gaussian white noise source with zero mean and correlation determined by the fluctuation−dissipation theorem:

$$\langle \xi(t)\xi(t')\rangle = 2k_B T\gamma_{th}\delta(t-t'). \tag{2}$$

In the presence of a stochastic potential, the friction constant must be renormalized to balance this additional noise in order to satisfy equipartition, especially in the low-friction regime where these contributions may become significant. This has presently been accomplished through a self-consistent procedure described previously,[31] in which $\gamma$ is renormalized according to the relation

$$\gamma^{(n+1)} = \gamma^{(n)}\left(\frac{\langle v^2(t)\rangle_n}{k_b T}\right), \tag{3}$$

at each $n$th iteration until convergence. An alternative that includes the spatial dependence of the friction has been derived based upon an extension of the fluctuation−dissipation theorem and is in preparation.[32] A criticism to the former approach lies in the approximation made in developing eq 3 in which $F(q,t)$ is treated as a local noise source obeying a fluctuation−dissipation relation equivalent to eq 2. However, the stochastic potentials have memory and are therefore nonlocal in nature leading to nonvanishing cumulants at third and higher orders. These effects are included, but only in an average manner, in the self-consistent approach and are ignored in the space-dependent approach all together. At this level of description, both methods are capable of capturing the essential dynamical effects.[32] Here, we will employ the simpler self-consistent approach.

The stochastic potential gives rise to a time-dependent force, $F(t) \equiv -\nabla_q U(q;t)$. In the model studies that follow, the form of the potential, $U(q;t)$, is either that of a set of merged harmonic oscillators (MHOs) or sinusoidal. The MHO potentials can be represented explicitly as

$$U(x;t) = \begin{cases} \frac{1}{2}k_0(x - x_m{}^0)^2 & \text{for } x_m{}^0 < x \le x_m^- \\ V_m^{\ddagger} + \frac{1}{2}k_m^{\ddagger}(x - x_m^{\ddagger})^2 & \text{for } x_m^- < x \le x_m^+ \\ \frac{1}{2}k_0(x - x_{m+1}^0)^2 & \text{for } x_m^+ < x \le x_{m+1}^0, \end{cases} \tag{4}$$

where the wells and barriers are centered at $x_m^0 = -\lambda/2 + m\lambda$ and $x_m^{\ddagger} = m\lambda$, respectively. The connection points are constructed to ensure continuity in the potential and its first derivative; this leads to the result $x_m^{\pm} = \pm k_0\lambda/(2k_0 - 2k_m^{\ddagger}) + m\lambda$. The width of the barriers varies stochastically in time according to the relation $k_m^{\ddagger} = -(k_0 + \eta(m,t))$. This, in turn, defines the barrier height $V_m^{\ddagger} = -k_0 k_m^{\ddagger}\lambda^2/(8k_0 - 8k_m^{\ddagger})$.

In this work, the two-dimensional sinusoidal potentials are given the simple form

$$U(x,y;t) = (2E_b + \eta(t))\left(\sin\left(\frac{2\pi x}{a}\right)\sin\left(\frac{2\pi y}{a}\right) + 1\right), \tag{5}$$

where the wells are connected by barriers along the diagonals, and the one-dimensional potentials are similarly defined as

$$U(x;t) = \left(E_b + \frac{1}{2}\eta(t)\right)\left(\sin\left(\frac{2\pi x}{b}\right) + 1\right). \tag{6}$$

The two have equivalent well-to-well distances if $b = a\sqrt{2}$. (See section 1 of the Appendix for the connection between eq 5 and the rectilinear form chosen in ref 6.) In both cases, $E_b$ is the barrier height, and $\eta(t)$ is an auxiliary stochastic variable. In the numerical investigations, the thermal energy is chosen so that it is $^1/_6$th of the average value of the barrier heights. The constant factors in the amplitudes are included to ensure

consistency between the barrier heights in the two models. In two dimensions, particles selectively escape over the saddles of the potential, as opposed to the one-dimensional case in which they are forced to traverse the maxima. As such, one can reference the values of the instanteous barrier height for both the one- and the two-dimensional potentials to the chosen temperature such that it has the values, $6k_bT + \eta(t)$.

As can be seen from the form of the equations above, these potentials fall into two general classes based upon the spatial correlations of the barrier heights. For instance, all of the barriers of the sinusoidal potential fluctuate in unison (i.e., coherently) with one another, whereas the barriers of the MHOs are capable of fluctuating independently (i.e., incoherently). Nonetheless, in the limit that the MHOs are forced to fluctuate coherently, the transport properties that it gives rise to are nearly identical to those found for the corresponding stochastic sinusoidal potential. Consequently, the numerical results for the one-dimensional coherent stochastic MHO potential have been omitted throughout this work. For simplicity, the one-dimensional stochastic *coherent* sinusoidal potential and *incoherent* MHO potential will be referred to as $1D_{sin}$ and $1D_{MHO}$, respectively. In addition to the two-dimensional coherent sinusoidal potential, a quasi-incoherent two-dimensional sinusoidal potential has also been included by allowing the barriers in the two respective dimensions to fluctuate independently of one another by including a stochastic variable for each dimension. These will henceforth be referred to as the coherent, $2D_C$, and incoherent, $2D_I$, potentials. A fully incoherent two-dimensional surface has been developed in which every barrier is allowed to fluctuate independently of all other barriers and is currently being tested.[32]

As mentioned previously, the stochastic features of these potentials are contained in $\eta(t)$, which is, in turn, defined as an Ornstein−Uhlenbeck process. It is described by the well-known stochastic differential equation

$$\dot{\eta} = -\frac{\eta}{\tau} + \sqrt{\frac{2\sigma^2}{\tau}}\,\zeta(t), \tag{7}$$

where $\sigma^2$ is the variance of the distribution, $\tau$ is the $\eta$-correlation time in the stochastic potential, and $\zeta(t)$ is an additional white noise term. As such, $\eta(t)$ has a probability distribution

$$P(\eta) = \frac{1}{\sqrt{2\pi\sigma^2}} \exp\left(-\frac{\eta^2}{2\sigma^2}\right), \tag{8}$$

and is correlated in time through the expression

$$\langle \eta(t)\eta(t')\rangle = \sigma^2 \exp\left(-\frac{|t-t'|}{\tau}\right). \tag{9}$$

Modification of $\tau$ allows one to control the extent of the exponentially decaying correlation in the barrier heights. Simulations are performed over 10 decades in the $\eta$-correlation time, $\tau$. In the lower limit, a fully random surface with variations in the barrier heights from one instant in time to the next is parametrized only by the variance. The higher limit essentially corresponds to the sampling of single realizations of the potential energy surface whose barrier heights are determined by the initial values of $\eta$ as chosen from the distribution given by eq 8.

The dynamics of these systems were characterized by the mean first passage time (MFPT) of a particle to escape from an initial minima of the potential. The corresponding rate for such a process is given by the inverse of this quantity. However, one must be cautious in defining when a particle has escaped from its initial well. A standard transition state approach is not adequate when considering this class of potentials because the barrier heights (and possibly positions) are not fixed. A method capable of accounting for this type of phenomena is the use of a geometrical constraint in the phase space of the Brownian particle.[33] More precisely, the criterion used to characterize a first passage process is defined as the time required for a particle to escape its present minima and stabilize with an energy $E \leq Dk_bT$ in another minima, where $D$ is the dimensionality of the system. The MFPT is thus defined as the average of the first passage times over all trajectories

$$\tau_{MFPT} \equiv \lim_{N\to\infty} \frac{1}{N} \sum_{i=1}^{N} \tau_{FPT}(i). \tag{10}$$

Stochastic trajectories were obtained by numerical integration of the coupled eqs 1 and 7 according to the method described by Ermak and Buckholtz.[34,35] For these simulations, the MFPT was seen to converge with respect to both the time step size and number of trajectories when their values were 0.001 and 10 000, respectively.

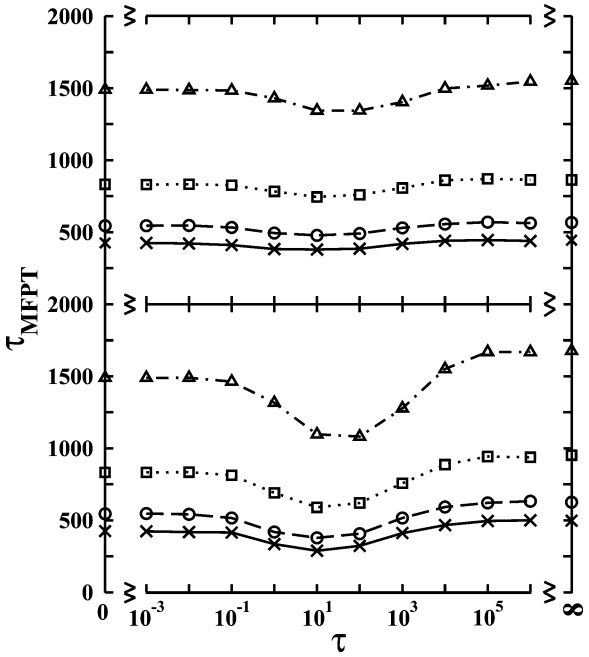


**Figure 1.** The MFPT versus the correlation time, $\tau$, at $k_BT = {}^2/_3$ (in units of some standard temperature $k_BT_0$) on the $2D_I$ potential in the overdamped regime for values of the friction constant, $\gamma_{th}$: 0.8 (solid curve and × symbols), 2 (dashed curve and circles), 4 (dotted curve and squares), and 8 (dot−dashed curve and triangles). The variance, $\sigma^2$, is equal to 0.2 and 0.6 in the top and bottom panels, respectively. The calculations for the MFPTs in the $\tau = 0$ and $\tau = \infty$ limits are described in the text and are presently displayed on the ordinates.

## III. Results and Discussion

As a first test of our approach, the dynamics were studied in the overdamped regime. This regime has been studied extensively over the past decade, largely due to the phenomenon known as resonant activation.[18] Depending on the $\eta$-correlation time, $\tau$, of the fluctuations of the potential, a minimum in the MFPT (maximum in the rate) is observed for these systems. The results for our simulations in the high friction regime are displayed in Figure 1 for the $2D_I$ potential, with the top and

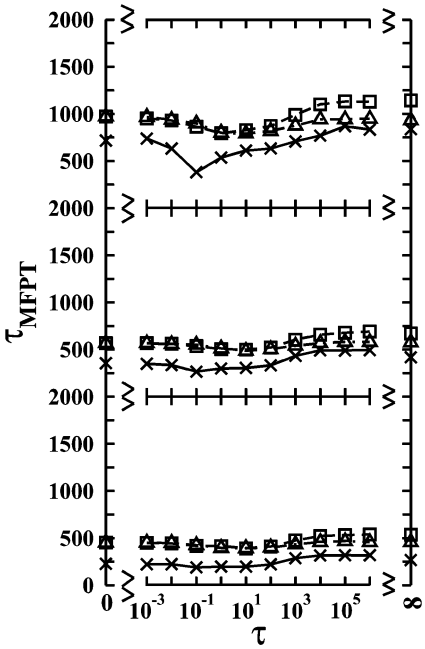


**Figure 2.** The MFPT versus the correlation time, $\tau$, in the underdamped regime for each of three potentials: $1D_{sin}$ (solid curve and × symbols), $2D_C$ (dashed curve and squares), and $2D_I$ (dot−dashed curve and triangles). The top, middle, and bottom panels represent results obtained at the values, 0.08, 0.2, and 0.4, of the friction constant, $\gamma_{th}$, respectively. The variance, $\sigma^2$, is equal to 0.2 and the well-to-well distance is $\sqrt{2}$ in all three cases. The limits displayed on the ordinates were obtained from numerical simulations as in Figure 1.

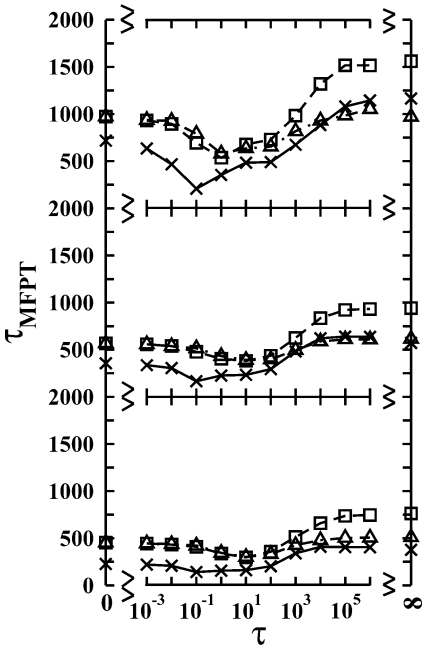


**Figure 3.** The MFPT versus the correlation time, $\tau$, for the same systems as described in Figure 2 but with the variance, $\sigma^2$, set to 0.6.

bottom panels representing two different values of the variance of the distribution given in eq 8. The correction to the friction constant due to the stochastic potentials is negligible compared with the large thermal component in this regime. The values at the ordinates represent the numerically calculated values of the MFPT for the $\tau = 0$ and $\tau = \infty$ limits. In the zero $\eta$-correlation time limit, the fluctuations in the potential are so rapid that the diffusive particle effectively experiences the average, stationary potential, from which the dynamics are computed. At the opposite limit, however, the barrier height is essentially a fixed value representing dynamics on a single realization of the surface whose magnitude is sampled from the distribution given by eq 8. As can be seen, the behavior of the MFPT calculated for intermediate values of the $\eta$-correlation time is approaching the respective limits, which lends weight to our physical understanding of the phenomenological prescription.

Until recently, these simulations have only been performed in the overdamped regime due to an inability to accurately describe the friction in the underdamped regime where additional dissipative factors must be included to maintain equipartition. Using the method described above for constructing this correction, we have extended these simulations into the low-friction regime. If there is no coupling between the two degrees of freedom (i.e., the passage time is simply related to the probability of escape), then the rate (inverse MFPT) on the two-dimensional surfaces should be twice that of the corresponding one-dimensional potential. Plotted in Figures 2 and 3 are the MFPTs for two values of the variance obtained for each of the three sinusoidal surfaces with those from the 1D model scaled by a factor of $^1/_2$ to test this hypothesis. The well-to-well distance is $\sqrt{2}$ for all three potentials. The top, middle, and bottom panels correspond to values of the friction constant of 0.08, 0.2, and 0.4, respectively. For low to intermediate values of the $\eta$-correlation time, $\tau$, the behavior of the MFPT on the one-dimensional potential essentially mirrors that of the two-dimensional coherent potential except for a constant shift to lower passage times that is invariant to changes in friction or variance. This can be attributed to topographical differences between the two surfaces. For example, in one dimension, the particle may surmount the barrier if it acquires enough energy, regardless of its corresponding direction of travel. However, the two-dimensional potentials include four areas of almost insurmountable energy that the particles must avoid in order to escape, thus increasing the passage time.

At low $\eta$-correlation time, the MFPTs for both of the two-dimensional potentials are coincident. This is the result one would expect because this regime corresponds to the dynamics of the average potential in which the two surfaces are equivalent. As $\tau$ is increased, and hence the surface behaves less like the average, the differences between the two-dimensional models become significant, especially when the variance of the distribution controlling the range of possible barrier heights is increased, as seen in Figure 3. In the case of the $2D_C$ stochastic potential, when $\tau$ is large, all four exit channels are described by the same barrier height, and hence a particle with insufficient energy to escape over one barrier cannot escape over any of the others. However, in the $2D_I$ stochastic potential, despite the presence of such an exit channel, the other exit channel will have a nonneglible probability of being described by a lower barrier height that gives rise to escape on a time scale shorter than $\tau$. Consequently, the incoherent potential can give rise to faster transport than the coherent potential for sufficiently large $\tau$. As the friction is reduced and hence the particle becomes more energetically limited, this phenomenon becomes more pronounced.

To explore the effects of coherent and incoherent barriers further, as well as the impact of lattice spacing, simulations were performed for the one- and two-dimensional sinusoidal surfaces as well as the fully incoherent MHO potential. The MFPTs for these four potentials are displayed in Figure 4. Again the top, bottom, and middle panels correspond to values of the thermal friction of 0.08, 0.2, and 0.4, respectively. The MFPTs obtained from the one-dimensional potentials are scaled by $^1/_2$ as in Figures 2 and 3. The lattice spacing for all of the potentials is

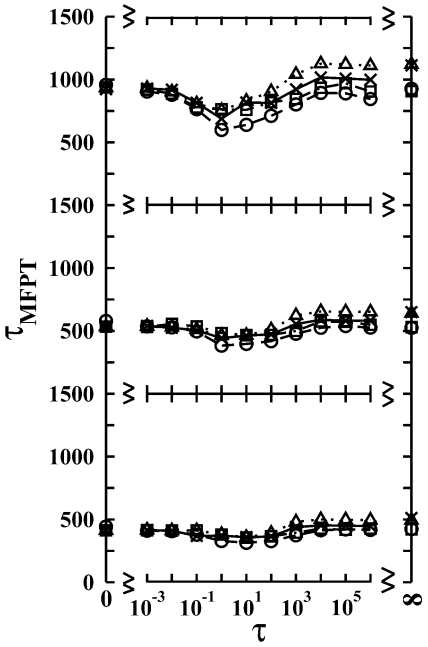


**Figure 4.** The MFPT for each of four stochastic potentials characterized by the variance, $\sigma^2 = 0.22$, and well-to-well distance equal to 4, but with all other parameters the same as in Figure 2. The corresponding potentials are $1D_{sin}$ (solid curve and × symbols), $2D_C$ (dotted curve and triangles), $2D_I$ (dot−dashed curve and squares), and $1D_{mho}$ (dashed curve and circles).

chosen as 4, and the variance is 0.22 to satisfy restrictions made by the MHO potential (see section 2 of the Appendix). As opposed to Figures 2 and 3, the small $\eta$-correlation time, $\tau$, behavior of all four potentials is equivalent. The results for the two-dimensional potentials are essentially unchanged from those of Figure 2, whereas the one-dimensional potentials are shifted to longer MFPTs. The only difference between Figure 2 and Figure 4 with respect to the dynamics across the corresponding stochastic potentials is an increase in the lattice spacing from $\sqrt{2}$ to 4. The resulting effects on the MFPT may be due to coupling of the 2 degrees of freedom in the two-dimensional potentials. Any energy acquired can be dissipated through either degree of freedom, whereas in one-dimension this is not possible. The two-dimensional potentials are then mostly energy diffusion-limited in which the lattice spacing will have a negligible effect. However, the diffusing particles on the one-dimensional surfaces do not have access to this mechanism, and therefore spatial diffusion effects can play a small, but noticeable effect. In the large $\tau$ regime, the MFPTs increase in the order $1D_{MHO} < 2D_I < 1D_{sin} < 2D_C$. In this regime, the two incoherent potentials diffuse at a faster rate than the coherent potentials as a result of the decoupled exit channels. Again, the effects of the four impassable areas of the two-dimensional potentials are reflected in their respective shifts to larger passage times.

The stochastic rate enhancement for the $1D_{sin}$, $2D_C$, and $2D_I$ potentials can be seen in Figures 5, 6, and 7, respectively, for a variance of 0.6. The top, middle, and bottom panels display the total rate, $\Gamma_\infty$, single hop rate, $\Gamma_1$, and multiple hop rate, $\Gamma_m \equiv (1 - \Gamma_1)$. Each is normalized with respect to the corresponding rate obtained from the average potential (i.e., the $\tau = 0$ limit). The rate enhancement is seen for all three potentials, although slightly larger in one dimension than in two dimensions. The effects of coherency play a small role as seen from the results of the $2D_C$ and $2D_I$ potentials, the latter providing a minor adjustment to the overall rate for most values of $\tau$. However, at large $\tau$, the rate of the coherent potential is

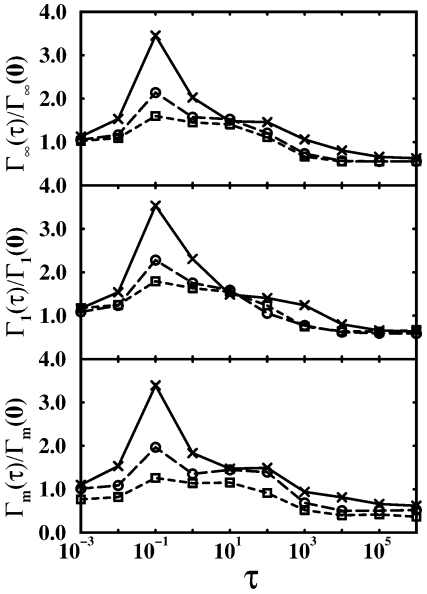


**Figure 5.** Hopping rates obtained on the $1D_{sin}$ potential normalized with respect to the corresponding rates obtained on the average potential displayed as a function of the correlation time, $\tau$, for a variance of $\sigma^2 = 0.6$ and values of the friction constants $\gamma_{th}$: 0.08 (solid curve and x symbols), 0.2 (dashed curve and circles), and 0.4 (dotted curve and squares). The top, middle, and bottom panels display the total rate, $\Gamma_\infty$, the single hopping rate, $\Gamma_1$, and the multiple hop rate, $\Gamma_m$, respectively.

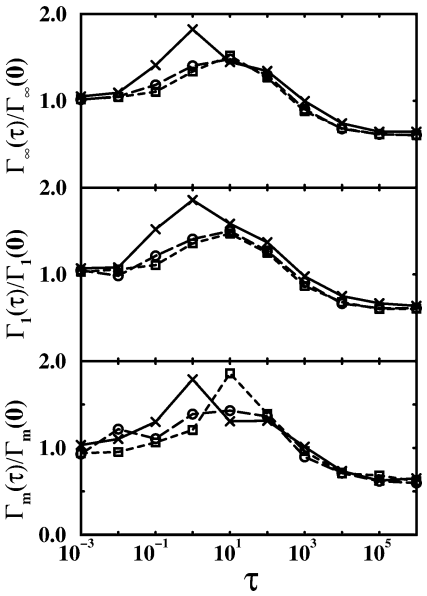


**Figure 6.** Normalized rates obtained from the $2D_C$ potential displayed as a function of the correlation time, $\tau$. All of the parameters are the same as those in Figure 5.

significantly lower than the average, whereas the incoherent potential is able to avoid this decrease due to the uncoupled exit channels. As can be seen from all three figures, the rate enhancements for single and multiple hops are roughly equal. Although not shown for brevity, the multiple hopping probabilities have also been calculated for all three potentials and follow the same trend. This is the expected result because the fluctuations in the barrier height are relatively small compared with the average and therefore should not enhance or impede a particle with sufficient energy to complete a multiple hop trajectory.

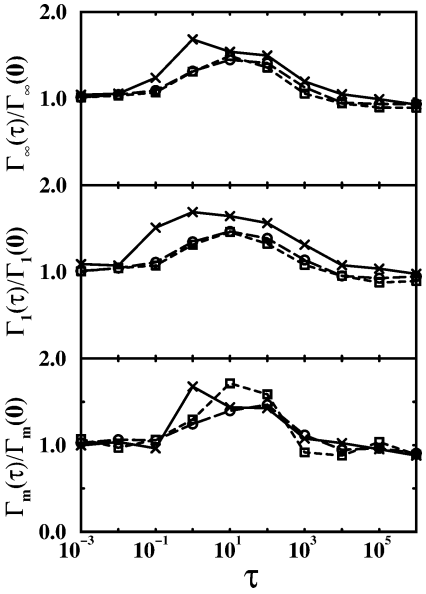


**Figure 7.** Normalized rates obtained from the $2D_I$ potential displayed as a function of the correlation time, $\tau$. All of the parameters are the same as those in Figure 5.

## IV. Concluding Remarks

This paper presents an application of a recent model that describes the diffusive behavior of a Brownian particle influenced by a stochastic potential of mean force in the low friction regime. An extension into this regime was necessary to adequately characterize the complicated process of surface diffusion. Here, we have provided some insights to the fundamental nature of this process. In particular, these simulations have revealed that the dynamics on one-dimensional potentials and the corresponding two-dimensional analogue are similar, except in the extreme limits of large $\tau$. Additionally, the results presented here are encouraging with regards to the ultimate goal of providing a new mechanism for patterning a surface by utilizing the dynamic range in the rates as modulated by $\tau$ in the barrier. This study has confirmed that the rate enhancement is observed in extended dimensions, follows a similar trend to the one-dimensional behavior, and in particular depends on $\tau$. The forthcoming application of the model will provide a more detailed study of incoherent, but prescribed, surfaces to see the extent to which patterns can emerge on a surface.[32]

## Appendix

**1. Sinusoidal Potentials.** The two-dimensional potential presented here is the same as that used in previous work on the diffusive motion on coupled and uncoupled stationary surfaces.[6] Although the form in eq 5 may at first glance appear coupled, a simple point transformation, rotating the coordinate frame by $\pi/4$, can be used to define the new coordinates, $u = x + y$ and $v = x - y$. This readily reduces eq 5 to

$$U(x,y;t) = (2E_b + \eta(t))[2 - \cos(v) - \cos(u)], \quad (11)$$

which is equivalent to the *nonstochastic* decoupled potential used in ref 6 when $\eta = 0$.

**2. Merged Harmonic Oscillators.** The barrier height for the MHO potentials is not given by a simple additive stochastic variable as with the sinusoidal potentials. As a consequence, the barrier height distribution, $P_{MHO}(V_m^\ddagger)$, is no longer given by eq 8. However, it can easily be determined according to

$$P_{MHO}(V_m^\ddagger) = P(\eta(V_m^\ddagger)) \frac{\partial \eta(V_m^\ddagger)}{\partial V_m^\ddagger} \quad (12)$$

where $\eta(V_m^\ddagger)$ is related to the barrier height as before. This distribution is both sharper and slightly skewed in comparison to the Gaussian distribution in $\eta$. Therefore, the stochastic sinusoidal potentials parametrized by $\eta$ with a variance of 0.2 and 0.6 correspond approximately to stochastic MHO barriers with a variance of 0.05 and 0.22, respectively. (The correspondence is due to the sharpening in the distribution, but it is approximate because the former is symmetric whereas the latter is slightly skewed.) Although it is possible to increase the variance in the random variable to yield stochastic MHO barrier heights with the large variances (e.g., 0.2 and 0.6) initially investigated using sinusoidal potentials in section III, it is not desirable because it leads to a significantly non-Gaussian distribution in the barrier heights. Moreover, this wide $\eta$ distribution contains a significant probability for inverse barriers, vis-à-vis wells, in which $k_m^\ddagger < 0$. (Note that when this probability is vanishingly small as in most of the cases in this work, the dynamics are not significantly affected.) Consequently, the parameters for the sinusoidal potentials were chosen to coincide with those of the stochastic MHO rather than the other way around.

**Acknowledgment.** This work has been partially supported by a National Science Foundation Grant, No. NSF 02-123320. R.H. is the Goizueta Foundation Junior Professor. The Center for Computational Science and Technology is supported through a Shared University Research (SUR) grant from IBM and Georgia Tech.

## References and Notes

(1) Georgievskii, Y.; Pollak, E. *Phys. Rev. E* **1994**, *49*, 5098.
(2) Bader, J. S.; Berne, B. J.; Pollak, E. *J. Chem. Phys.* **1995**, *102*, 4037.
(3) Tully, J. C. *Annu. Rev. Phys. Chem.* **2000**, *51*, 153.
(4) Yan, T.; Hase, W.; Tully, J. *J. Chem. Phys.* **2004**, *120*, 1031.
(5) Senft, D. C.; Ehrlich, G. *Phys. Rev. Lett.* **1995**, *74*, 294.
(6) Chen, L. Y.; Baldan, M. R.; Ying, S. C. *Phys. Rev. B* **1996**, *54*, 8856.
(7) Pedersen, M. Ø.; Österlund, L.; Mortensen, J. J.; Mavrikakis, M.; Hansen, L. B.; Stensgaard, I.; Lægsgaard, E.; Nørskov, J. K.; Besenbacher, F. *Phys. Rev. Lett.* **2000**, *84*, 4898.
(8) Swartzentruber, B. S. *Phys. Rev. Lett.* **1996**, *76*, 459.
(9) Schunack, M.; Linderoth, T. R.; Rosei, F.; Lægsgaard, E.; Stensgaard, I.; Besenbacher, F. *Phys. Rev. Lett.* **2002**, *88*, 156102.
(10) Oh, S. M.; Kyuno, K.; Koh, S. J.; Ehrlich, G. *Phys. Rev. B* **2002**, *66*, 233406.
(11) Jardine, A.; Ellis, J.; Allison, W. *J. Phys.: Condens. Matter* **2002**, *14*, 6173.
(12) Tully, J.; Gilmer, G.; Shugard, M. *J. Chem. Phys.* **1979**, *71*, 1630.
(13) Shepherd, T.; Hernandez, R. *J. Phys. Chem. B* **2002**, *106*, 8176.
(14) Linderoth, T. R.; Horch, S.; Lægsgaard, E.; Stensgaard, I.; Besenbacher, F. *Phys. Rev. Lett.* **1997**, *78*, 4978.
(15) Tully, J. C. *J. Chem. Phys.* **1980**, *73*, 1975.
(16) Tully, J. C. *Surf. Sci.* **1982**, *111*, 461.
(17) Benzi, R.; Sutera, A.; Vulpiani, A. *J. Phys. A* **1981**, *14*, L453.
(18) Doering, C. R.; Gadoua, J. C. *Phys. Rev. Lett.* **1992**, *69*, 2318.
(19) Reimann, P.; Hänggi, P. In *Stochastic Dynamics*; Schimansky-Geier, L., Poschel, T., Eds.; Lecture Notes in Physics; Springer: Berlin, 1997; Vol. 484, pp 127−139.
(20) Pollak, E.; Bader, J.; Berne, B. J.; Talkner, P. *Phys. Rev. Lett.* **1993**, *70*, 3299.
(21) Hershkovitz, E.; Talkner, P.; Pollak, E.; Georgievski, Y. *Surf. Sci.* **1999**, *421*, 73.
(22) Talkner, P.; Hershkovitz, E.; Pollak, E.; Hänggi, P. *Surf. Sci.* **1999**, *437*, 198.

(23) Astumian, R.; Moss, F. *Chaos* **1998**, *8*, 533.
(24) Gammaitoni, L.; Hänggi, P.; Jung, P.; Marchesoni, F. *Rev. Mod. Phys.* **1998**, *70*, 223.
(25) Zhang, X. P.; Bao, J. D. *Surf. Sci.* **2003**, *540*, 145.
(26) Jansch, H.; Xu, J.; J. T. Yates, J. *J. Chem. Phys.* **1993**, *99*, 721.
(27) Ditchfield, R.; Llera-Rodriguez, D.; Seebauer, E. *Phys. Rev. Lett.* **1998**, *81*, 1259.
(28) Whitman, L. J.; Stroscio, J. A.; Dragoset, R. A.; Celotta, R. J. *Science* **1991**, *251*, 1206.
(29) Shklyaev, A. A.; Shibata, M.; Ichikawa, M. *J. Appl. Phys.* **2000**, *88*, 1397.
(30) Shklyaev, A. A.; Shibata, M.; Ichikawa, M. *J. Vac. Sci. Technol., B* **2001**, *19*, 103.
(31) Shepherd, T.; Hernandez, R. *J. Chem. Phys.* **2001**, *115*, 2430.
(32) Moix, J.; Hernandez, R. Unpublished results.
(33) Shepherd, T.; Hernandez, R. *J. Chem. Phys.* **2002**, *117*, 9227.
(34) Ermak, D. L.; Buckholz, H. *J. Comput. Phys.* **1980**, *35*, 169.
(35) Allen, M. P.; Tildesley, D. J. *Computer Simulations of Liquids*; Oxford: New York, 1987.